16th World Conference on Earthquake, 16WCEE 2017

Santiago Chile, January 9th to 13th 2017

Paper N° 2606

Registration Code: S-F1461865547

REVIEW OF LABORATORY TEST DATA FOR COMBINED LATERAL AND GRAVITY SHEAR DEMANDS ON INTERIOR SLAB-COLUMN CONNECTIONS

Y. Zhou[(1)], M.D. Hueste[(2)]

[(1)] *Graduate Student, Zachry Department of Civil Engineering, Texas A&M University, College Station, TX, USA, zhou3023@tamu.edu*
[(2)] *Professor, Zachry Department of Civil Engineering, Texas A&M University, College Station, TX, USA, mhueste@tamu.edu*

Abstract

Flat slabs are a common floor system for commercial and residential buildings. Past earthquake damage has shown that slab-column (SC) frames are not a suitable main lateral-force-resisting system in regions of high seismic risk because of their relative flexibility and potential for brittle punching shear failures. However, SC frame systems are common lateral systems in regions of low-to-moderate seismic risk, as well as gravity systems in regions of high seismic risk where moment frames or shear walls are provided as the main lateral-force-resisting system. In such cases, SC connections must still maintain sufficient strength and ductility to resist gravity loads under the presence of inelastic deformations. In the last several decades, the two-way shear response of SC connections has been evaluated by a significant number of experiments. These experiments provide physical tests to examine and calibrate design methods. However, details for these tests can be difficult to obtain and differences in defining key response parameters can lead to inconsistencies in some of the summarized test results. In addition, design recommendations have in some cases been developed based upon a limited subset of the available laboratory test data that did not include more recent tests. To avoid these limitations, this paper documents a database of SC connection tests that uses consistent criteria for selecting key response parameters. The collected test results include interior reinforced concrete SC connections with and without shear reinforcement under combined lateral and gravity shear demands. The relationship between the limiting drift and gravity shear ratio is examined for the data. The laboratory test data are investigated with respect to the load simulation technique, failure mode, shear reinforcement, and slab span-to-thickness ratio. The laboratory test data relating limiting drift to gravity shear demand data is compared to the current ACI 318-14 relationship for evaluating the design lateral deformation demands for SC connections in Seismic Design Categories D, E, and F. Because of the importance of the gravity shear demand on the SC connection, influence of flexural reinforcement ratio, and slab thickness; this paper also summarizes provisions for determining the nominal two-way shear strength provided by the concrete in three building codes: ACI 318-14, JSCE 15, and Eurocode 2 (2004). The differences in the estimated two-way shear strength provided by ACI 318-14 versus the Japanese and European codes are reviewed for select specimens, and the impact of these differences on the computed gravity shear ratio is evaluated.

Keywords: reinforced concrete; slab-column connections; shear reinforcement; design codes; experimental database

1. Introduction

Flat slabs are a common floor system for commercial and residential buildings. Past earthquake damage has shown that slab-column (SC) frames are not a suitable main lateral-force-resisting system (LFRS) in regions of high seismic risk because of their relative flexibility and potential for brittle punching shear failures. However, SC frame systems are common LFRSs in regions of low-to-moderate seismic risk, as well as gravity systems in regions of high seismic risk where moment frames or shear walls are provided as the main LFRS. In such cases, the reinforced concrete (RC) SC connections must still maintain sufficient strength and ductility to resist gravity loads under the presence of inelastic deformations.

Slab-column connections experience very complex behavior when subjected to lateral displacements or unbalanced gravity loads. The portion of the slab around the column must transfer a combination of shear, flexure, and torsion. Flexural and diagonal cracking of the slab are coupled with significant in-plane compressive forces induced by the restraint of the surrounding unyielding portions of the slab. The first punching shear design specification in the US was introduced by the Joint Committee on Concrete and Reinforced Concrete in 1912 [1]; a maximum value for punching shear stress was given. In 1963, the ACI 318 Building Code first required the investigation of punching shear stress due to unbalanced moment caused by gravity, wind, or earthquake demands [2]. The "eccentric shear stress model" used in the ACI Building Code is based on the work by DiStasio and Van Buren [3] and reviewed by ACI-ASCE Committee 326 [4].

Experiments have been conducted over the past forty years to evaluate the performance of SC connections under the combined effects of gravity and lateral loading. These tests have indicated a relationship between the limiting lateral drift ratio (*DR*) and the gravity shear ratio (*VR*) that can be used for deformation compatibility checks. *VR* is defined as the ratio $V_{ug} / (\phi V_c)$ where the term V_c is the nominal shear strength provided by the concrete, and $\phi = 0.75$ for design [5]. The factored gravity shear force, V_{ug}, is determined using the load combinations of $1.2D + 1.0L$ (or $0.5L$) $+ 0.2S$ as specified in ACI 318-14 [5], where D, L, and S are the dead, live, and snow loads, respectively. It is not possible for *VR* to be equal to or greater than unity for connections without shear reinforcement, as the factored gravity shear V_u for $1.2D + 1.6L$ ($> V_{ug}$) is always less than ϕV_c.

ACI 318-05 [6] incorporated a simplified relationship between *DR* and *VR* that is used to evaluate the design lateral deformation demand for SC connections not designated as part of the seismic-force-resisting system in structures assigned to Seismic Design Categories (SDCs) D, E, and F; where DR = larger of [$(0.035 - 0.05VR)$ and 0.005]. Further, ACI 318 requires shear reinforcement to be provided for SC connections if the design story drift exceeds *DR*. In such cases, the shear stress capacity (v_s) provided by shear reinforcement must satisfy $v_s \geq 3.5\sqrt{f_c'}$, where f_c' is the concrete compressive strength (psi units). Also, the shear reinforcement must extend at least $4h$ away from, and perpendicular to, the face of the support, drop panel, or column capital; where h is the slab thickness. These criteria are still in place in ACI 318-14.

Experiments in the literature provided physical tests to examine and calibrate design methods. However, details for these tests can be difficult to obtain and differences in defining key response parameters can lead to inconsistencies in some of the summarized test results. In addition, design recommendations have in some cases been developed based upon a limited subset of the available laboratory test data. To avoid these limitations, this paper provides a review of the database of interior RC SC connection tests using a consistent criteria for selecting key response parameters. The collected test results include interior RC connections with and without shear reinforcement under combined lateral and gravity shear demands. This paper also compares design provisions for determining V_c for three building codes to determine the impact on the computed *VR* for the SC specimens.

2. Review of Available Research

2.1 Typical SC specimen test setup

Most experiments evaluating SC connections under gravity load with lateral displacement have tested individual SC connections or portions of a structure containing SC connections. It is critical to choose a test setup that is able to realistically model the effect of loads and deformations on the connection. Fig. 1 depicts three typical methods of load application for individual RC SC connections. These specimens include a column section extended on both sides of the slab and terminated at the assumed points of contraflexure for lateral load. The slab is typically square in plan and extended to the inflection points, which is equivalent to the midspan location of the prototype structure, in the lateral loading direction. Three methods of gravity load application have been used for these specimens [1]:

- application of a concentrated axial load through the column (i.e., column jacking) (Fig. 1b),
- application of distributed point loads to the slab around the connection (Fig. 1c), or
- a combination of both methods (Fig. 1a).

In some cases an initial axial load is applied to the top of the column to induce a typical axial load while *VR* is maintained through the application of distributed loading to the slab. In such cases, the gravity load application to the SC connection is noted below as being consistent with Fig. 1c.

Methods to induce unbalanced moments at the SC connection include:

- application of lateral displacements at the top of the column with the base fully fixed or restrained against translation and with slab edges roller supported (Fig. 1a),
- application of lateral displacements at both column ends with slab edges simply supported (Fig. 1b), or
- application of an upward and downward displacement couple at opposite edges of the slab with both ends of the column restrained (Fig. 1c).

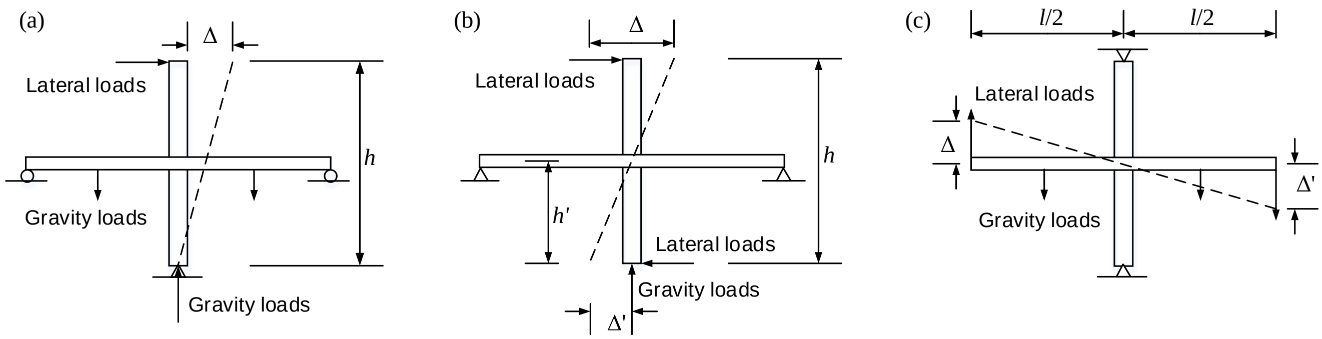

Fig. 1 – Typical load simulation for individual interior SC connection specimens

There are potential concerns with inducing gravity load using column jacking, as shown in Fig. 1b. For this case, the initial gravity shear in the connection region is equal to the applied column load as intended. Upon the application of a lateral load, the slab shear force on one side of the column will increase, while decreasing on the other side of the column by the same amount. As testing continues and yielding occurs on one side of the SC connection, the gravity load will tend to shift from the SC connection to one of the slab supports. So, while the assumed *VR* is present without lateral load, it may be much less than assumed during lateral load testing. This leads to challenges with maintaining the intended *VR* at the connection.

2.2 Key parameters and modes of failure

The laboratory test data was reviewed using a consistent methodology, and key parameters were determined for each test. The actual gravity shear ratio *VR* is determined as $V_g/\phi V_c$, where V_g is the reported direct shear force transferred at the critical shear perimeter, V_c is calculated in accordance with ACI 318-14 Sect. 22.6.5.2 using the reported measured material properties and geometry, and ϕ=1.0. The failure mode for each specimen is categorized as punching shear *(P)*, flexure *(F)*, or a combination of flexure and punching shear (*FP*) where a punching shear failure occurred at a higher drift level following yielding of the slab reinforcement.

The drift ratio (*DR*) is defined as the ratio of column lateral displacement to the column height, or the ratio of slab displacement to slab length. For the application of unbalanced moments shown in Fig. 1c, the slab deflections on either side of the column were not equal for most tests. *DR* was therefore determined by Eq. (1).

$$DR = [\Delta/(l/2) + \Delta'/(l/2)] / 2 \tag{1}$$

Fig. 2 depicts the measured lateral load versus drift ratio relationships for four specimens under reversed uniaxial cyclic lateral loads. The selected specimens exhibit a wide range of behaviors for the database of RC SC connection tests. "*DR* at peak load" corresponds to the lateral drift at the maximum (peak) applied lateral load; "*DR* limit" corresponds to the lateral drift ratio at which failure occurs (*P*, *FP*, or *F*) or when the lateral load drops to 80% of its peak value. If the test was terminated prior to any of these events, the mode is noted as no failure (*NF*). The *DR* at peak load and the *DR* limit are not necessarily identical, as Fig. 2 indicates.

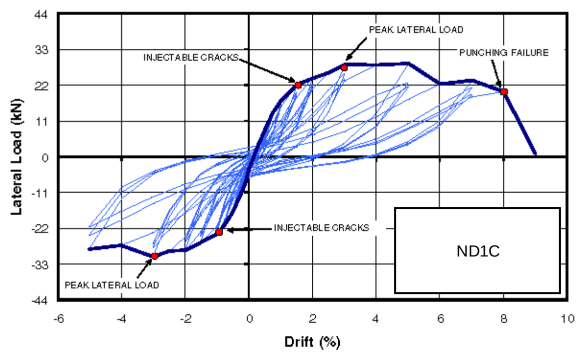

(a) Flexure-punching failure (*FP*) [7]
DR at peak load: +3.00% / -3.00%
DR limit: 8.00%

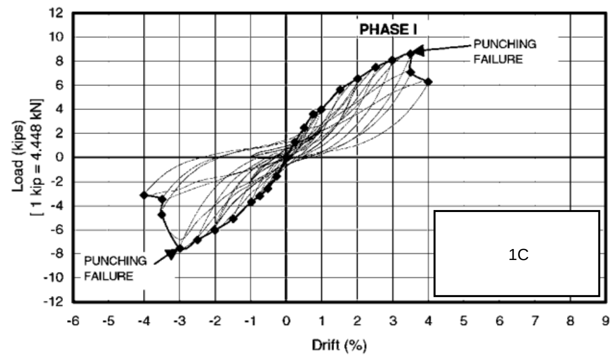

(b) Punching failure (*P*) [8]
DR at peak load: +3.50% / -3.00%
DR limit: 3.25%

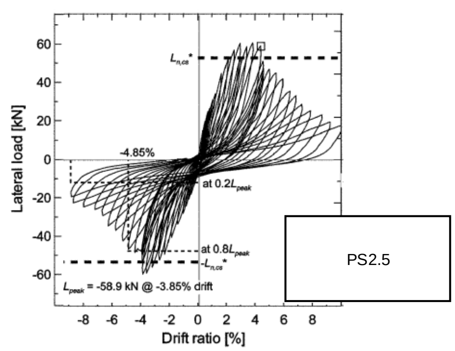

(c) Flexure failure (*F*), adapted from [9]
DR at peak load: +3.85% / -3.85%
DR limit: 4.85% (80% of peak load)

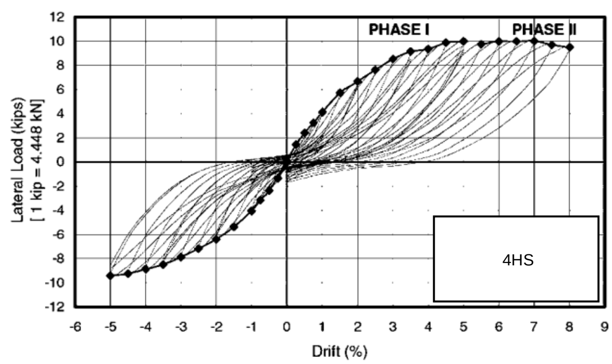

(d) Flexure failure (*F*) [8]
DR at peak load: +5.00% / -5.00%
DR limit: 8.00%

Fig. 2 – Examples of *DR* at peak load and *DR* limit (1 kN = 0.2248 kips)

Fig. 2 illustrates some specific examples for interpreting *DR* limit, as follows.

- When a *P* or *FP* failure occurred only in the positive or negative lateral load direction, the value of the *DR* limit corresponds to that failure point (see Fig. 2a).
- When a *P* or *FP* failure occurred in both the positive and negative lateral load directions, the *DR* limit is taken as the average of the drift ratios corresponding to both failure points (see Fig. 2b).
- For specimens that failed by flexure (*F*) or did not fail (*NF*), the *DR* limit is the greater drift value for both lateral load directions. *DR* limit is either the drift corresponding to 80% of the peak lateral load or the drift at which testing was terminated. Fig. 2c shows that the ultimate lateral load is below 80% of the peak lateral load in both directions; therefore, the *DR* limit is the point corresponding to the 80% of peak lateral load in the direction having the greater drift value.

- Fig. 2d shows an example of a flexure failure, as well; however, the ultimate lateral load is greater than 80% of the peak lateral load in both directions. The *DR* limit of this specimen is taken as the larger drift ratio corresponding to the end of test.

For specimens subjected to bidirectional lateral loads, the *DR* limit is reported as resultant drift ratios. In each principal vector direction, the *DR* limit is determined as noted above for unidirectional lateral load. To compare with tests under unidirectional lateral loads, the resultant *DR* limit is found as shown in Eq. (2),

$$DR = \sqrt{DR_x^2 + DR_y^2} \tag{2}$$

where DR_x and DR_y are the *DR* limit values corresponding to the two principal lateral loading directions.

2.3 Summary of laboratory test specimens

The reviewed database includes the available laboratory test data for RC SC connections under combined gravity and lateral loads. Included are 83 interior RC SC connections without shear reinforcement (Table 1) and 66 interior RC SC connections with shear reinforcement (Table 2).

Table 1 – Test data for interior slab-column connection specimens with no shear reinforcement

Source	**ID**	***VR***	***DR*, %**	**Mode**	**Source**	**ID**	***VR***	***DR*, %**	**Mode**
Hanson and Hanson (1968) [10]	B7	0.04	3.80	P	Robertson (1990) [17]	1	0.17	3.00	NF
	C8	0.05	5.80	P		2C	0.18	5.00	F
Hawkins et al. (1974) [11]	S1	0.34	1.84	P		3SE	0.15	4.00	FP
	S2	0.45	1.07	P		5SO	0.17	3.25	P
	S3	0.43	1.23	P		6LL	0.52	0.85	P
	S4	0.41	2.05	P		7L	0.37	1.45	P
Ghali et al. (1976) [12]	SM 0.5	0.31	6.50	FP		8I	0.18	4.50	F
	SM 1.0	0.33	2.70	P	Cao (1993) [18]	CD1	0.85	1.04	P
	SM 1.5	0.30	2.00	P		CD5	0.64	1.26	P
Islam and Park (1976) [13]	1	0.25	4.44	P		CD8	0.51	1.48	P
	2	0.23	5.00	P	Du (1993) [19]	DNY_1*	0.20	4.50	F
	3C	0.24	5.19	P		DNY_2*	0.30	2.00	P
Symonds et al. (1976) [14]	S-6	0.87	0.83	P		DNY_3*	0.24	4.50	F
	S-7	0.80	0.47	P		DNY_4*	0.28	4.70	FP
	S-8	0.62	0.64	F	Farhey et al. (1993) [20]	1	0.00	5.60	FP
Morrison and Sozen (1981) [15]	S1	0.03	4.83	F		2	0.00	5.10	FP
	S2	0.03	2.84	F		3	0.26	3.80	FP
	S3	0.04	4.29	F		4	0.30	2.50	FP
	S4	0.09	4.29	FP	Luo et al. (1994) [21]	II*	0.08	5.00	F
	S5	0.17	4.65	FP	Ali and Alexander (2002) [22]	SP-A	0.31	4.50	FP
Zee and Moehle (1984) [16]	interior	0.29	3.50	FP		SP-B	0.31	3.50	P

Table 1 – Test data for interior RC slab-column connection specimens with no shear reinforcement (cont.)

Source	ID	*VR*	*DR*, %	Mode	Source	ID	*VR*	*DR*, %	Mode
Hwang (1989) [23]	b2[bi]	0.24	4.47	P	Emam et al. (1997) [28]	HHHC05	0.25	5.20	F
	c2[bi]	0.26	4.85	P		HHHC10	0.25	5.20	FP
	b3[bi]	0.25	5.00	P		NHHC05	0.35	3.80	FP
	c3[bi]	0.26	5.32	P		NHHC10	0.36	3.80	P
Pan and Moehle (1988) [24]	AP1	0.37	1.54	FP	Robertson et al. (2002) [8]	1C	0.15	3.25	P
	AP2[bi]	0.36	1.83	FP	Brown (2003) [29]	SJB-6	0.45	2.30	P
	AP3	0.18	4.76	FP		SJB-7	0.51	1.70	P
	AP4[bi]	0.18	3.56	FP	Tian et al. (2008) [30]	L0.5*	0.23	2.00	P
Tan and Teng (2005) [25]	YL-L1	0.17	7.10	F		LG0.5*	0.23	1.25	NF
	YL-H2[bi]	0.28	2.39	P		LG1.0*	0.23	1.25	NF
	YL-L2[bi]	0.17	2.81	P	Park et al. (2012) [31]	RC-A	0.45	1.50	FP
Robertson and Johnson (2006) [26]	ND1C*	0.22	8.00	FP		RC-B	0.41	1.60	FP
	ND4LL*	0.27	3.50	FP	Song et al. (2012) [32]	RC1	0.43	1.80	P
	ND5XL*	0.44	2.00	P	Kang et al. (2013) [33]	RC	0.40	2.60	FP
	ND6HR*	0.27	4.00	P	Fick et al. (2014) [34]	Floor 1	0.21	2.39	NF
	ND7LR*	0.24	5.00	FP		Floor 2	0.21	3.31	P
	ND8BU*	0.24	5.00	FP		Floor 3	0.21	3.08	NF
Choi et al. (2007) [27]	S1	0.30	3.00	P	Rha et al. (2014) [35]	LM-S2-C5	0.40	5.38	FP
	S2	0.50	3.00	P		LM-S3-C5	0.40	0.74	FP
	S3	0.30	3.00	P		LC-S2-C5	0.40	1.50	P
Kang and Wallace (2008) [9]	C0	0.30	1.85	P	-	-	-	-	-

*Bottom slab reinforcement is discontinuous at interior connection; [bi] Biaxial lateral loading.
F = flexural failure, *P* = punching shear failure, *FP* = flexural and punching shear failure, *NF* = no failure

Table 2 – Test data for interior RC slab-column connection specimens with shear reinforcement

Source	ID	*VR*	*DR*, %	Mode	Shear Reinf.	Source	ID	*VR*	*DR*, %	Mode	Shear Reinf.
Hawkins et al. (1975) [36]	SS1	0.40	3.89	F	Closed stirrup	Islam and Park (1976) [13]	4S	0.23	5.37	P	Bent up
	SS2	0.38	4.44	P	Closed stirrup		5S[+]	0.23	4.63	F	Shear head
	SS3	0.39	5.76	F	Closed stirrup		6CS[+]	0.24	4.44	F	Closed stirrup
	SS4	0.38	5.63	F	Closed stirrup		7CS[+]	0.24	4.07	F	Closed stirrup
	SS5	0.34	5.00	FP	Closed stirrup		8CS[+]	0.27	5.56	F	Closed stirrup

Table 2 – Test data for interior RC slab-column connection specimens with shear reinforcement (cont.)

Source	ID	*VR*	*DR*, %	Mode	Shear Reinf.	Source	ID	*VR*	*DR*, %	Mode	Shear Reinf.
Symonds et al. (1976) [14]	SS-6	0.82	1.59	FP	Closed stirrup	Broms (2007) [39]	17c	0.65	3.00	FP	Ductility reinf.
	SS-7	0.81	2.25	FP	Closed stirrup		17d	0.65	3.00	FP	Ductility reinf.
Robertson (1990) [17]	4S	0.16	7.00	F	Closed stirrup		18c	0.67	3.00	FP	SSR
Cao (1993) [18]	CD3	0.90	3.41	FP	SSR		18d	0.67	3.00	FP	SSR
	CD4	0.61	4.81	F	SSR	Kang and Wallace (2008) [9]	PS2.5	0.32	4.85	F	Shear bands
	CD6	0.68	4.89	F	SSR		PS3.5	0.34	3.45	FP	Shear bands
	CD7	0.50	5.19	F	SSR		HS2.5	0.31	5.20	P	SSR
Dechka (2001) [37]	S1	0.46	4.40	P	SSR	Park et al. (2012) [31]	LR-A1	0.44	7.00	F	Lattice
	S2	0.47	6.40	FP	SSR		LR-A2	0.44	4.90	F	Lattice
Robertson et al. (2002) [8]	2CS	0.14	8.00	F	Closed stirrup		SR-A	0.45	4.00	F	SSR
	3SL	0.09	8.00	F	Single stirrup		SB-A	0.45	5.10	F	Shear bands
	4HS	0.13	8.00	F	SSR		ST-A	0.45	3.00	F	Stirrup
Brown (2003) [29]	SJB-1	0.48	4.50	FP	SSR		LR-B1	0.41	4.70	F	Lattice
	SJB-2	0.46	4.90	FP	SSR		LR-B2	0.41	3.60	F	Lattice
	SJB-3	0.48	4.90	FP	SSR		SR-B	0.41	5.10	F	SSR
	SJB-4	0.43	6.40	FP	SSR		SB-B	0.41	6.50	F	Shear bands
	SJB-5	0.47	7.60	FP	SSR		ST-B	0.41	3.20	F	Stirrup
	SJB-8	0.46	5.70	FP	SSR	Song et al. (2012) [32]	SR1	0.43	3.90	F	Stirrup
	SJB-9	0.49	7.10	FP	SSR		SR2	0.43	5.40	F	SSR
Tan and Teng (2005) [25]	YL-H2V^{bi}	0.28	5.60	FP	SSR		SR3	0.43	6.00	F	Shear bands
	YL-H1V	0.28	8.14	F	SSR	Kang et al. (2013) [33]	LR-A	0.40	5.10	F	Lattice
Gayed and Ghali (2006) [38]	ISP-0	0.84	3.76	FP	SSR		LR-B	0.40	3.20	FP	Lattice
Cheng (2009) [1]	SU1	0.42	5.00	F	SFR		LR-C	0.40	4.80	F	Lattice
	SU2	0.33	5.00	F	SFR		LR-D	0.40	5.10	F	Lattice
	SB1^{bi}	0.40	3.25	P	SFR		LR-E	0.40	3.60	FP	Lattice
	SB2^{bi}	0.41	2.95	P	SFR	Matzke et. al. (2015) [40]	B1^{bi}	0.45	2.62	FP	SSR
	SB3^{bi}	0.43	1.46	P	SSR		B2^{bi}	0.45	2.62	FP	SSR
-	-	-	-	-	-		B3^{bi}	0.47	2.95	FP	SSR
-	-	-	-	-	-		B4^{bi}	0.41	3.25	FP	SSR

*Bottom slab reinforcement is discontinuous at interior connection; ^{bi} Biaxial lateral loading, $^{+}$ *DR* was based on the slab displacement at peak lateral load as the author reported.
F = flexural failure, *P* = punching shear failure, *FP* = flexural and punching shear failure, *NF* = no failure

The majority of test specimens are individual interior RC SC specimens, as depicted in Fig. 1. In addition, a limited number of tests have been conducted with multi-connection specimens, multi-panel specimens, and multi-story frame specimens. The multi-connection specimen is a two-bay-one-story frame that contains two exterior and one interior connections, tested by Robertson [17], Du [19], and Dechka [37]. The multi-panel specimen includes two types: a nine-panel, one-story frame specimen tested by Hwang [23] and a four-panel, one-story frame specimen tested by Rha et al. [35]. A full-scale three-story flat-plate structure was tested by Fick et al. [34].

Table 3 summarizes the reviewed database in terms of the method of lateral load (or unbalanced moment) and gravity load application. The designations “a,” “b,” and “c” refer to the setups shown in Fig. 1a, 1b, and 1c, respectively. Among the three basic loading setups, the test configuration and lateral load simulation in Fig. 1a is the most popular. Test specimens subject to induced unbalanced moments using the approach shown in Fig. 1a have an applied gravity load using one of the three methods described earlier. Differences in tests also include monotonic versus cyclic lateral loading, unidirectional versus bidirectional loading, and some specimens include the effects of continuity with a multiple panel or frame setup. All tests are unidirectional unless noted otherwise.

Table 3 – Load simulation of interior RC SC connections

<table>
<tr><th>Lateral Load</th><th>Gravity Load</th><th>Lateral Load Type</th><th>Sources</th><th>Notes</th></tr>
<tr><td rowspan="4">a</td><td>a</td><td>Cyclic</td><td>[24, 25]</td><td rowspan="2">[24, 25] included biaxial tests
[24] included both type a and b gravity load</td></tr>
<tr><td>b</td><td>Cyclic</td><td>[9, 15, 24, 30, 31, 32, 33, 39]</td></tr>
<tr><td rowspan="2">c</td><td>Cyclic</td><td>[1, 8, 16, 17, 19, 21, 22, 23, 26, 34, 35, 37, 40]</td><td rowspan="2">[1, 40] included biaxial tests
[17, 19, 37] are multi-connection tests
[23] was a biaxial multi-panel test
[34] was a three-story frame test
[35] was a multi-panel test with 2 monotonic and 1 cyclic specimens</td></tr>
<tr><td>Monotonic</td><td>[35]</td></tr>
<tr><td rowspan="2">b</td><td rowspan="2">b</td><td>Cyclic</td><td>[12, 18, 20, 27, 28, 29, 38]</td><td rowspan="2">[12] included 3 monotonic specimens
[29] included 1 monotonic specimen</td></tr>
<tr><td>Monotonic</td><td>[12, 29]</td></tr>
<tr><td rowspan="2">c</td><td rowspan="2">c</td><td>Cyclic</td><td>[11, 13, 14, 36]</td><td rowspan="2">[10] included 2 monotonic specimens
[13] included 4 monotonic specimens</td></tr>
<tr><td>Monotonic</td><td>[10, 13]</td></tr>
</table>

2.4 Relationship between limiting drift and gravity shear ratio

The relationship between the *DR* limit and *VR* for interior RC SC connections with and without shear reinforcement is shown in Fig. 3. As shown in Fig. 3a, most test specimens without shear reinforcement failed by punching. All *FP* failure points had a *VR* below 0.5, and most *F* and NF points had a *VR* less than 0.3. Fig. 3b shows the *DR* limit versus *VR* for specimens with different types of shear reinforcement. Typical shear reinforcement includes shear stud reinforcement (SSR), closed stirrups, bent-up bars, and shearheads. More recently, several new types of shear reinforcement including “ductility reinforcement,” shearbands, steel fiber reinforcement (SFR), and lattice reinforcement were tested, as noted in Table 2. Fig. 3b shows that no tests have been conducted for shear reinforced RC SC connections with *VR* ranging from 0.5-0.6 and 0.7-0.8. Many tests have been conducted with SSR, particularly in the range of *VR* = 0.4-0.5; however, the *DR* limit is highly variable.

Fig. 4a and Fig. 4b show the influence of the different load simulation techniques on *DR* limit as a function of *VR*. The labels a, b, and c correspond to the test configuration and lateral load simulation of Fig. 1a, 1b, and 1c; respectively. To eliminate effects from other factors, the data included in these graphs are limited to: (1) individual interior RC SC connections under uniaxial lateral loading, (2) specimens with continuous bottom slab reinforcement, and (3) specimens with column sections extended above and below the slab and ended at the assumed points of contraflexure. Although there is significant scatter in the data, a best-fit line is included for each set of data to provide a simple estimate of the overall trends. Fig. 4a for RC SC connections with no shear reinforcement indicates that type b gravity and lateral load simulation corresponds to a slightly higher drift capacity than for tests using type a or c load simulation. Fig. 4b for RC SC connections with shear reinforcement shows a stronger trend for higher *DR* limits for a given *VR* under type b load simulation. A number of factors may contribute to the observed increase in the *DR* limit (i.e., type and amount of shear reinforcement, flexural reinforcement ratio, slab effective depth, and span-to-depth ratio); however, it is interesting to note the overall increase in the *DR* limit considering the challenges in maintaining the intended *VR* with this test setup.

The tendency for the *DR* limit for SC connections to decrease as *VR* increases limits the application of flat-plate structures in high seismic regions, as well as for buildings with high gravity loads. One approach to enhance the shear resistance and drift capacity of SC connections is to add shear reinforcement. Fig. 5 compares the lateral response of RC SC connections with and without shear reinforcement. It is noted that the presence of shear reinforcement typically enhances the lateral displacement ductility of SC connections for varying levels of *VR*. The chart shows the drift limit relationship provided in ACI 318-14 for SC connections not designated as part of the seismic-force-resisting system in structures assigned to SDCs D, E, and F, as discussed earlier.

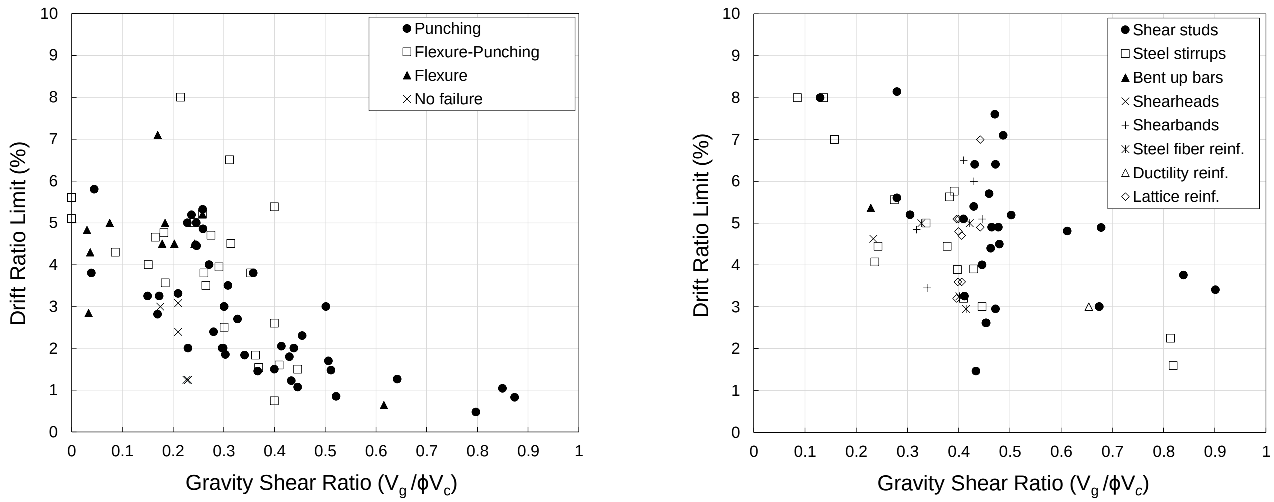

(a) Connections without shear reinforcement (b) Connections with shear reinforcement

Fig. 3 – Reviewed data for RC interior connections

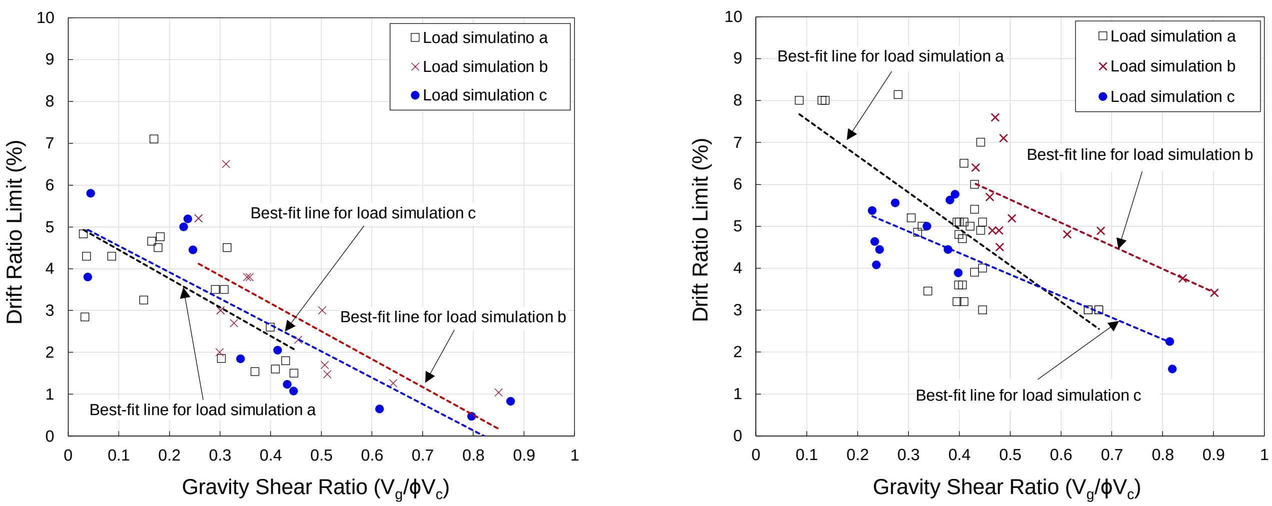

(a) Connections without shear reinforcement (b) Connections with shear reinforcement

Fig. 4 – Load simulation for individual connections

The span-to-thickness ratio of slabs was reviewed with respect to the type of load simulation. Fig. 6 shows the span-to-thickness ratio (l_1/h) for specimens, where l_1 is the slab dimension in the direction of loading and h is the slab thickness. The reviewed data in Fig. 6 met the same criteria used for developing the plots in Fig. 4. The labels a, b, and c correspond to the test configuration and lateral load simulation of Fig. 1a, 1b, and 1c; respectively. Fig. 6 shows that the slab span-to-thickness ratio (l_1/h) for specimens with type b load simulation tends to be lower than for the other two types. The lower l_1/h is more typical of cases with a higher *VR* as the slab inflection point is likely to be closer to the connection [41]. Lower l_1/h values makes SC connections less flexible, which means the expected drift capacity for type b load simulation is lower than for type a and c. However, Fig. 4a and Fig. 4b show the opposite trend. While other parameters may contribute, the issues with maintaining *VR* with the use of column jacking, as in type b load simulation, could be a factor.

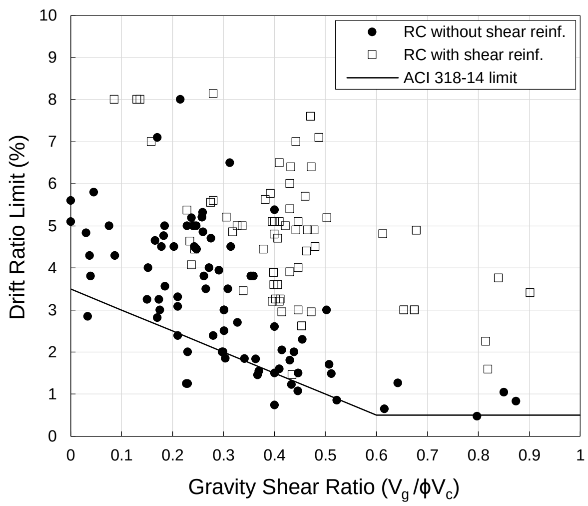

Fig. 5 – Reviewed data for RC interior connections

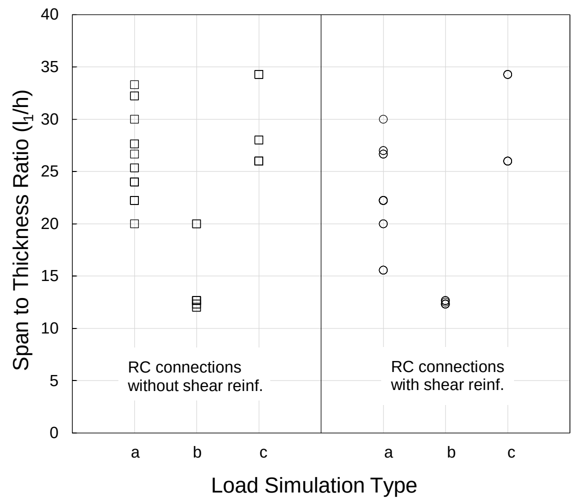

Fig. 6 – l_1/h versus load simulation type

3. Building Code Provisions

The provisions for determining nominal shear strength provided by concrete V_c for interior SC connections without shear reinforcement are summarized in Table 4 for three building codes and the ACI 352.1R-11 recommendations.

Table 4 – Provisions for V_c

Code	b_o	V_c	Size effect	Reinforcement effect
ACI 318-14 [5] ACI 352.1R-11 [42] (US units)	c, c, $0.5d$ $b_o = 4(c+d)$	$4\sqrt{f_c'}b_o d$	—	—
JSCE 15 [43] (SI units)	c, c, $0.5d$ $b_o = 4c + \pi d$	$0.20\sqrt{f_c'}\beta_d\beta_p\beta_r b_o d/\gamma_b$	$\beta_r = 1 + \frac{1}{1+0.25u/d}$ $\beta_d = \sqrt[4]{1000/d} \le 1.5$	$\beta_p = \sqrt[3]{100\rho}$ $\beta_p \le 1.5$
Eurocode 2 [44] (SI units)	c, c, $2d$ $b_o = 4(c+\pi d)$	$\frac{0.18}{\gamma_c}\sqrt[3]{100\rho f_{ck}}kb_o d$	$k = 1 + \sqrt{\frac{200}{d}} \le 2.0$	$\sqrt[3]{100\rho}$ $\rho \le 0.02$

Note: f_c' is specified compressive strength of concrete, MPa (psi for US units); f_{ck} is characteristic concrete cylinder compressive strength, MPa; $f_{ck} = f_c'$-1.6 MPa [45]; γ_b and γ_c are member factor and partial factor for concrete and are taken as 1.0; b_o is perimeter of critical section, mm (in. for US units); d is average effective depth, mm (in. for US units); c is column dimension, mm (in. for US units); u is perimeter of column, mm; ρ is average reinforcement ratio in two principal directions.

The expressions provided in Table 4 consider only square columns and normal-weight concrete. The difference between each provision is the perimeter of critical section for shear b_o (column 2), the size effect (column 4), and the effect of slab flexural reinforcement (column 5). JSCE 15 and Eurocode 2 include the slab flexural reinforcement ratio as a parameter in estimating V_c, whereas ACI 318-14 does not. Fig. 7a shows the normalized estimated two-way shear strength, $V_{c\text{-}code}/V_{c\text{-}ACI\ 318\text{-}14}$, as a function of ρ_{c2+3h} for interior SC connections without shear reinforcement; where ρ_{c2+3h} is the slab flexural reinforcement ratio within a width of c_2+3h, and c_2 is the column dimension transverse to the loading direction. As expected, the normalized estimated two-way shear strength increases as the flexural reinforcement ratio increases for both the JSCE 15 and Eurocode 2. The ACI 318-14 estimates of V_c are lower for slabs with a ρ_{c2+3h} greater than 0.8% and 1.3% for the JSCE 15 and Eurocode 2, respectively. As such, ACI 318-14 provides larger estimates of V_c for lightly reinforced slabs. The JSCE 15 V_c estimates are higher than those for the Eurocode 2 for all reinforcement ratios. Fig. 7b depicts the relationship of *DR* limit versus *VR* computed for each of the three codes. Although their estimation of two-way shear strength varies, all three codes show a similar trend.

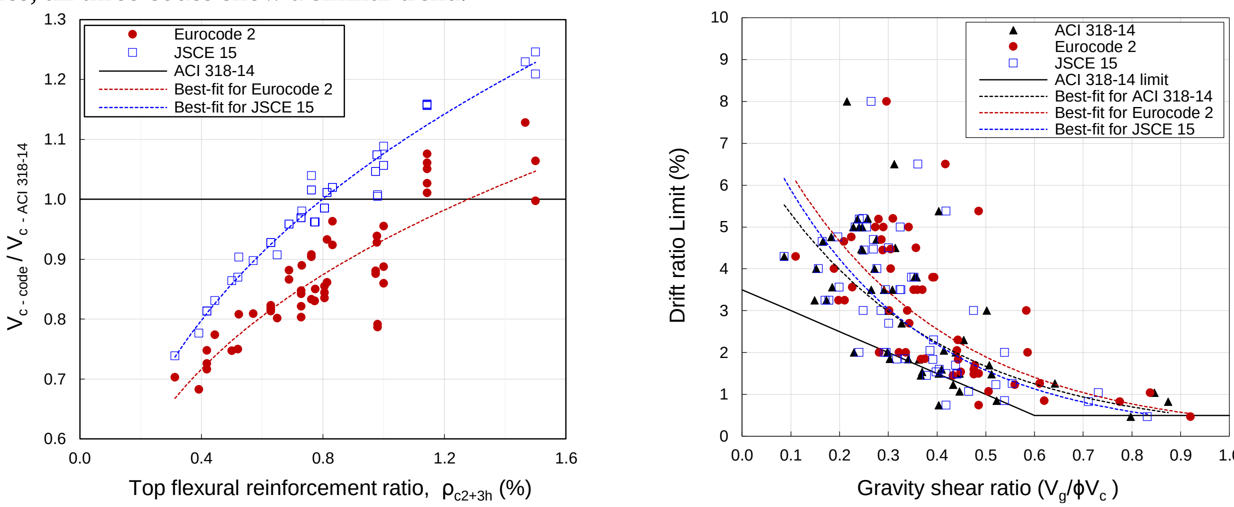

(a) Estimated two-way shear

(b) *DR* limit versus *VR*

Fig. 7 –Reviewed data of interior SC connections without shear reinforcement due to different codes

4. Conclusions

Based on the detailed review of available tests for RC SC interior connections with and without shear reinforcement under combined lateral and gravity shear loading, the following conclusions are made.

1) Most RC SC specimens without shear reinforcement failed by punching. All *FP* failure points had a *VR* below 0.5, and most *F* and NF points had a *VR* less than 0.3. The updated laboratory test data set confirms that the *DR* limit tends to decrease as *VR* increases, which is the basis for the ACI 318-14 limiting drift relationship. However, there is significant variation in the *DR* limit for a given *VR*.
2) In general, the presence of shear reinforcement improves the lateral displacement ductility of RC SC connections for varying levels of *VR*. However, the *DR* limit is highly variable among these tests. No tests are available for RC SC connections with shear reinforcement with *VR* ranging from 0.5-0.6 and 0.7-0.8.
3) Tests of SC connections using type b load simulation include specimens with lower l_1/h ratios than for type a and c load simulation, however the higher drift capacity was observed for type b loading. Although a number of factors may contribute to the observed increase in drift capacity, it is noted that type b load simulation may lead to overestimating the limiting drift of RC SC connections.
4) Compared to Eurocode 2 and JSCE 15, which consider the effect of flexural reinforcement ratio on two-way shear strength (V_c), ACI 318-14 gives larger estimates of V_c for lightly reinforced interior SC connections. However, the flexural reinforcement ratio did not have a significant influence on the relationship of *DR* limit versus *VR* for the reviewed laboratory test data.

5. References

[1] Cheng M. Y. (2009): Punching shear strength and deformation capacity of fiber reinforced concrete slab-column connections under earthquake-type loading. *Ph.D. Dissertation*, University of Michigan, Ann Arbor, 347 pp.

[2] ACI Committee 318 (1963): Building code requirements for reinforced concrete. *ACI 318-63*, American Concrete Institute (ACI), Detroit, MI.

[3] Di Stasio J, Van Buren MP (1960): Transfer of bending moment between flat plate floor and column. *ACI Journal Proceedings*, **57**(9), 299-314.

[4] ACI-ASCE Committee 326 (1962): Report of ACI-ASCE committee 326-shear and diagonal tension: Part 1, Part 2, and Part 3. *Journal of American Concrete Institute* (ACI).

[5] ACI Committee 318 (2014): Building code requirements for structural concrete and commentary. *ACI 318-14*, American Concrete Institute (ACI), Farmington Hills, MI.

[6] ACI Committee 318 (2005): Building code requirements for structural concrete and commentary. *ACI 318-05*, American Concrete Institute (ACI), Farmington Hills, MI.

[7] Robertson IN, Johnson GP (2004): Non-ductile slab-column connections subjected to cyclic lateral loading, *Proceedings of 13WCEE*, Vancouver, Canada.

[8] Robertson IN, Kawai T, Lee J, Enomoto B (2002): Cyclic testing of slab-column connections with shear reinforcement. *ACI Structural Journal*, **99**(5), 605-613.

[9] Kang TH, Wallace JW (2008): Seismic performance of reinforced concrete slab-column connections with thin plate stirrups. *ACI Structural Journal*, **105**(5), 617-625.

[10] Hanson NW, Hanson JM (1968): Shear and moment transfer between concrete slabs and columns. *Journal, PCA Research and Development Laboratories*, **10**(1), 2-16.

[11] Hawkins NM, Mitchell D, Sheu MS (1974): Cyclic behavior of six reinforced concrete slab-column specimens transferring moment and shear. *Progress report 1973-74*, Division of Structures and Mechanics, Department of Civil Engineering, University of Washington.

[12] Ghali A, Elmasri MZ, Dilger W (1976): Punching of flat plates under static and dynamic horizontal forces. *ACI Journal Proceedings*, **73**(10), 566-572.

[13] Islam S, Park R (1976): Tests on slab-column connections with shear and unbalanced flexure. *Journal of the Structural Division*, **102**(3), 549-568.

[14] Symonds DW, Hawkins NM, Mitchell D (1976): Slab-column connections subjected to high intensity shears and transferring reversed moments. *Technical Report SM 76-2*, Division of Structures and Mechanics, Department of Civil Engineering, University of Washington.

[15] Morrison DG, Sozen MA (1981): Response of reinforced concrete plate-column connections to dynamic and static horizontal loads, volume 1. *Technical Report to NSF*, University of Illinois Engineering Experiment Station. College of Engineering. University of Illinois at Urbana-Champaign.

[16] Zee HL, Moehle JP (1984): Behavior of interior and exterior flat plate connections subjected to inelastic load reversals. *Technical Report to NSF*, University of California, Earthquake Engineering Research Center.

[17] Robertson IN (1990): Seismic response of connections in indeterminate flat-slab subassemblies. *Ph.D. Dissertation*, Rice University, Houston, 278 pp.

[18] Cao HJ (1993): Seismic design of slab-column connections. *Masters Dissertation*, Univ. of Calgary, Alberta, 201 pp.

[19] Du Y (1993): Seismic resistance of slab-column connections in non-ductile flat-plate buildings. *Ph.D. Dissertation*, Rice University, Houston, 166 pp.

[20] Farhey DN, Adin MA, Yankelevsky DZ (1993): RC flat slab-column subassemblages under lateral loading. ASCE *Journal of Structural Engineering*, **119**(6), 1903-1916.

[21] Luo YH, Durrani AJ, Conte JP (1994): Equivalent frame analysis of flat plate buildings for seismic loading. ASCE *Journal of Structural Engineering*, **120**(7), 2137-2155.

[22] Ali MA, Alexander SD (2002): Behaviour of slab-column connections with partially debonded reinforcement under cyclic lateral loading. *Structural Engineering Report No. 243*, Department of Civil Engineering, University of Alberta.

[23] Hwang S (1989): An experimental study of flat-plate structures under vertical and lateral loads. *Ph.D. Dissertation*, University of California, Berkeley, 278 pp.

[24] Pan A, Moehle JP (1988): Reinforced concrete flat plates under lateral loading: an experimental study including biaxial effects. *Report to the National Science Foundation*, University of California, Berkeley.

[25] Tan Y, Teng S (2005): Interior slab-rectangular column connections under biaxial lateral loadings. *ACI Special Publication*, **232**, 147-174.

[26] Robertson I, Johnson G (2006): Cyclic lateral loading of nonductile slab-column connections. *ACI Structural Journal*, **103**(3), 356-364.

[27] Choi MS, Cho IJ, Han BS, Ahn JM, Shin SW (2007): Experimental study of interior slab-column connections subjected to vertical shear and cyclic moment transfer. *Key Engineering Materials*, **348**, 641-644.

[28] Emam M, Marzouk H, Hilal MS (1997): Seismic response of slab-column connections constructed with high-strength concrete. *ACI Structural Journal*, **94**, 197-205.

[29] Brown SJ (2003): Seismic response of slab column connections. *Ph.D. Dissertation*, Univ. of Calgary, Alberta, 341 pp.

[30] Tian Y, Jirsa JO, Bayrak O, Argudo JF (2008): Behavior of slab-column connections of existing flat-plate structures. *ACI Structural Journal*, **105**(5), 561-569.

[31] Park HG, Kim YN, Song JG, Song SM (2012): Lattice shear reinforcement for enhancement of slab-column connections. ASCE *Journal of Structural Engineering*, **138**(3), 425-437.

[32] Song JK, Kim J, Kim HB, Song JW (2012): Effective punching shear and moment capacity of flat plate-column connection with shear reinforcements for lateral loading. *International Journal of Concrete Structures and Materials*, **6**(1), 19-29.

[33] Kang SM, Park HG, Kim YN (2013): Lattice-reinforced slab-column connections under cyclic lateral loading. *ACI Structural Journal*, **110**(6), 929-939.

[34] Fick DR, Sozen MA, Kreger ME (2014): Cyclic lateral load test and the estimation of elastic drift response of a full-scale three-story flat-plate structure. *ACI Special Publication*, **296**, 1-14.

[35] Rha C, Kang TH, Shin M, Yoon JB (2014): Gravity and lateral load-carrying capacities of reinforced concrete flat plate systems. *ACI Structural Journal*, **111**(4), 753-764.

[36] Hawkins NM, Mitchell D, Hanna SN (1975): The effects of shear reinforcement on the reversed cyclic loading behavior of flat plate structures. *Canadian Journal of Civil Engineering*, **2**(4), 572-582.

[37] Dechka DC (2001): Response of shear -stud -reinforced continuous slab -column frames to seismic loads. *Ph.D. Dissertation*, University of Calgary, Canada, pp. 472.

[38] Gayed RB, Ghali A (2006): Seismic-resistant joints of interior columns with prestressed slabs. *ACI Structural Journal*, **103**(5), 710-719.

[39] Broms CE (2007): Flat plates in seismic areas: comparison of shear reinforcement systems. *ACI Structural Journal*, **104**(6), 712-721.

[40] Matzke EM, Lequesne RD, Parra-Montesinos GJ, Shield CK (2015): Behavior of biaxially loaded slab-column connections with shear studs. *ACI Structural Journal*, **112**(3), 335-346.

[41] Kang THK, Robertson IN, Hawkins NM, LaFave JM (2008): Recommendations for design of post-tensioned slab-column connections subjected to lateral loading. *Journal of the Post-Tensioning Institute*, **6**(1), 45-59.

[42] ACI-ASCE Committee 352 (2011): Guide for design of slab-column connections in monolithic concrete structures. ACI *352.1R-11*, American Concrete Institute (ACI), Farmington Hills, MI.

[43] JSCE 2010 Concrete Committee (2010): *JSCE No.15*-standard specification for concrete structures-2007 “Design”. Japan Society of Civil Engineers, Tokyo, Japan.

[44] British Standards Institution (2004): *Eurocode 2*: design of concrete structures: part 1-1: general rules and rules for buildings. British Standards Institution.

[45] Widianto, Bayrak O, Jirsa JO (2009): Two-way shear strength of slab-column connections: Reexamination of ACI 318 provisions. *ACI Structural Journal*, **106**(2), 160-170.